



A hypertension-associated mitochondrial DNA mutation introduces an m¹G37 modification into tRNA^{Met}, altering its structure and function

Received for publication, October 13, 2017, and in revised form, November 13, 2017. Published, Papers in Press, December 8, 2017, DOI 10.1074/jbc.RA117.000317

Mi Zhou^{#S1}, Ling Xue^{#1}, Yaru Chen^{#1}, Haiying Li^{#1}, Qiufen He^S, Bibin Wang^{#1}, Feilong Meng^{#S}, Meng Wang^{#S}, and Min-Xin Guan^{#S***#2}

From the [#]Division of Medical Genetics and Genomics, The Children's Hospital, Zhejiang University School of Medicine, Hangzhou, 310058 Zhejiang, China, the ^SInstitute of Genetics, Zhejiang University School of Medicine, Hangzhou, 310058 Zhejiang, China, the ¹Attardi Institute of Mitochondrial Biomedicine and the ^{#1}Department of Cardiology, the First Affiliated Hospital, Wenzhou Medical University, Wenzhou, 325035 Zhejiang, China, the ^{**}Collaborative Innovation Center for Diagnosis and Treatment of Infectious Diseases, Zhejiang University, Hangzhou, 310058 Zhejiang, China, and the ^{**}Joining Institute of Genetics and Genomic Medicine between Zhejiang University and University of Toronto, Hangzhou, 310058 Zhejiang, China

Edited by Ronald C. Wek

Defective nucleotide modifications of mitochondrial tRNAs have been associated with several human diseases, but their pathophysiology remains poorly understood. In this report, we investigated the pathogenic molecular mechanism underlying a hypertension-associated 4435A→G mutation in mitochondrial tRNA^{Met}. The m.4435A→G mutation affected a highly conserved adenosine at position 37, 3' adjacent to the tRNA's anticodon, which is important for the fidelity of codon recognition and stabilization. We hypothesized that the m.4435A→G mutation introduced an m¹G37 modification of tRNA^{Met}, altering its structure and function. Primer extension and methylation activity assays indeed confirmed that the m.4435A→G mutation created a tRNA methyltransferase 5 (TRMT5)-catalyzed m¹G37 modification of tRNA^{Met}. We found that this mutation altered the tRNA^{Met} structure, indicated by an increased melting temperature and electrophoretic mobility of the mutated tRNA compared with the wildtype molecule. We demonstrated that cybrid cell lines carrying the m.4435A→G mutation exhibited significantly decreased efficiency in aminoacylation and steady-state levels of tRNA^{Met}, as compared with those of control cybrids. The aberrant tRNA^{Met} metabolism resulted in variable decreases in mitochondrial DNA (mtDNA)-encoded polypeptides in the mutant cybrids. Furthermore, we found that the m.4435A→G mutation caused respiratory deficiency, markedly diminished mitochondrial ATP levels and membrane potential, and increased the production of reactive oxygen species in mutant cybrids. These results demonstrated that an aberrant m¹G37 modification of mitochondrial tRNA^{Met} affected the structure and function of its tRNA and consequently altered mito-

chondrial function. Our findings provide critical insights into the pathophysiology of maternally inherited hypertension, which is manifested by the deficient tRNA nucleotide modification.

Defects in nucleotide modifications of mitochondrial tRNAs have been associated with several clinical abnormalities including cancer, diabetes, neurological disorders, deafness, and hypertension (1–4). These nucleotide modifications of human 22 mitochondrial tRNAs encoded by its own genome were catalyzed by tRNA-modifying enzymes encoded by nuclear genome (5–8). To date, 15 types of modifications have been identified in 118 positions in different mammalian mitochondrial tRNAs (9, 10). These nucleotide modifications play a vital role in the structure and function of tRNAs (11–14). Core modifications including pseudouridylation at position 55 at the TΨC loop primarily contributed to structural stability of tRNAs and in some cases, may affect the aminoacylation (2, 3). These were exemplified by our recent discovery that the loss of pseudouridylation at position 55 at the TΨC loop of tRNA^{Glu} caused the maternally inherited deafness and diabetes (4). Indeed, the anticodon loop modifications including nucleotides at positions 34 and 37 regulate the stabilization of anticodon structure, fidelity, and efficiency of translation (2, 3, 11, 15–17). The defective 5-taurinomethyluridine (m⁵U) at U34 of tRNA^{Leu(UUR)} was associated with mitochondrial encephalopathy lactic acidosis and stroke-like episodes, whereas the lack of 5-taurinomethyl-2-thiouridine (m^{5s}2U) at U34 of tRNA^{Lys} was responsible for myoclonus epilepsy associated with ragged red fibers (MERRF) (18–20). Furthermore, mutations in tRNA modifying enzymes TRMU, MTO1, GTPBP3, and NSUN3 involved in nucleotide modifications at position 34 of mitochondrial tRNAs have been associated several clinical phenotypes including deafness (21–25).

The nucleotides at position 37 (A or G) of 17 mammalian mitochondrial tRNAs carry the diverse species of modifications, whereas no nucleotide modification at this position was detected in 5 tRNAs, such as tRNA^{Met} and tRNA^{Asp} (9). In fact, modifications of nucleotides A37 and G37 in human mitochon-

This work was supported by National Basic Research Priorities Program of China Grant 2014CB541704 (to M. X. G.), National Natural Science Foundation of China Grant 81600326 (to M. Z.), Postdoctoral Science Foundation of China Grant 2016M591987 (to M. Z.), and Fundamental Research Funds for the Central Universities Grant 2017QNA7026 (to M. Z.). The authors declare that they have no conflicts of interest with the contents of this article.

This article contains Fig. S1 and Tables S1 and S2.

¹ Both authors contributed equally to this work.

² To whom correspondence should be addressed: Institute of Genetics, Zhejiang University School of Medicine, Hangzhou, Zhejiang 310058, China. Tel.: 571-88206916; Fax: 571-88982377; E-mail: gminxin88@zju.edu.cn.

Hypertension-linked mitochondrial tRNA^{Met} mutation

drial tRNAs were catalyzed by the modifying enzymes TRIT1 and TRMT5 encoded by nuclear genes, respectively (8, 26, 27). The modifications at position 37 contributed to the high fidelity of codon recognition and to the structural formation and stabilization of functional tRNAs (11, 15, 26, 27). The defective i⁶A37 or m¹G37 modifications caused by mutations in the TRIT1 or TRMT5 were responsible for mitochondrial dysfunction leading to clinical phenotypes (26, 27). Mutations in the nucleotides at position 37 including the tRNA^{Ile} 4295A→G, tRNA^{Asp} 7551A→G, and tRNA^{Met} 4435A→G mutations were associated with hypertension, diabetes, visual loss, and deafness (28–33). In particular, the tRNA^{Met} 4435A→G mutation was identified in four genetically unrelated Chinese families with maternal transmission of hypertension (31–33). Therefore, it was hypothesized that the substitution of A with G at position 37 of the tRNA^{Met} may introduce the m¹G37 modification catalyzed by TRMT5, thereby altering the structure and function of tRNA^{Met}. In particular, the m.4435A→G mutation may affect the aminoacylation capacity and stability of tRNA^{Met} and then impair mitochondrial translation. It was also anticipated that defective mitochondrial translation caused by the m.4435A→G mutation alters the respiration, production of ATP and reactive oxygen species (ROS).³ To further investigate the pathogenic mechanism of the m.4435A→G mutation, cybrid cell lines were generated by transferring mitochondria from lymphoblastoid cell lines derived from an hypertensive matrilineal relative carrying the mutation and from a control subject lacking the mtDNA mutation but belonging to the same mtDNA haplogroup, into human mtDNA-less (ρ^0) cells (34, 35). Using these cell lines, we investigated if the m.4435A→G mutation introduced the m¹G37 modification of tRNA^{Met} by primer extension and methylation activity assays. These cell lines were then assessed for the effects of the m.4435A→G mutation on the stability and aminoacylation capacity of tRNA^{Met}, mitochondrial translation, enzymatic activities of electron transport chain complexes, the rate of O₂ consumption, ATP, and oxidative reactive species (ROS) as well as mitochondrial membrane potential.

Results

The m.4435A→G mutation created the m¹G37 modification of tRNA^{Met}

Neither i⁶A37 nor t⁶A37 modification was detected in the mammalian mitochondrial tRNA^{Met} (9). To investigate if the m.4435A→G mutation introduced the m¹G37 modification of tRNA^{Met}, we subjected mitochondrial RNAs from mutant and control cybrid cell lines to the reverse transcription with a digoxigenin (DIG)-labeled oligonucleotide probe specific for tRNA^{Met} (Fig. 1A). This resulted in a stop band one residue 3' to the methylation on 15% polyacrylamide gel. As shown in Fig. 1B, the m¹G37 modification was present in tRNA^{Met} derived from three mutant cell lines. However, the m¹G37 modification was not detected in the tRNA^{Met} derived from three control cell lines.

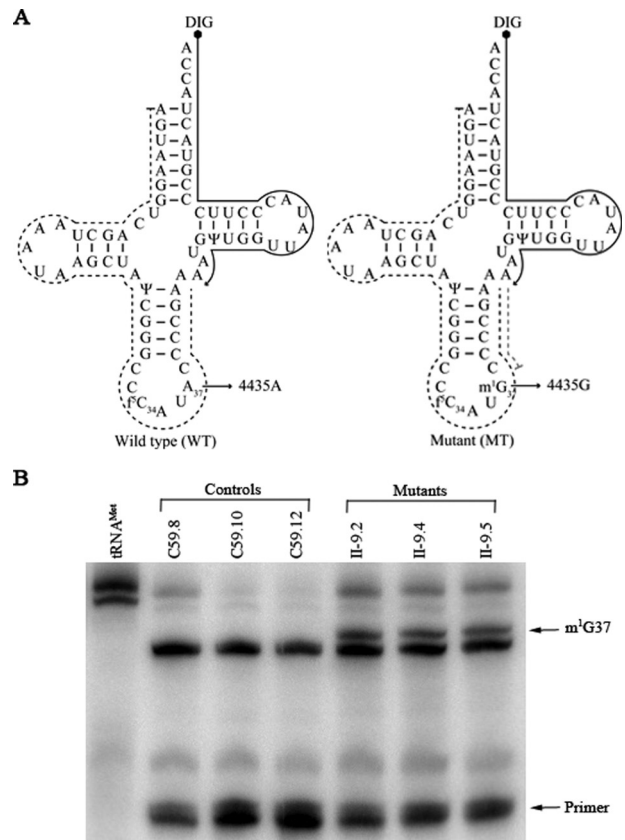


Figure 1. The m.4435A→G mutation created the m¹G37 modification of tRNA^{Met}. A, cloverleaf structure of human mitochondrial tRNA^{Met}. Arrows indicate the location of the m.4435A→G mutation. Solid lines represent the DIG-labeled oligonucleotide probe specific for tRNA^{Met}. Broken lines represented the potential stops of primer extension caused by the m¹G37 modification. B, primer extension demonstrated the creation of m¹G37 in the tRNA^{Met} carrying the m.4435A→G mutation. The primer extension termination products caused by m¹G37 modification are showed.

Methanocaldococcus jannaschii Trm5 (Mj-Trm5) catalyzed the m¹G37 modification in mutant tRNA^{Met} transcripts

Trm5 is one of the tRNA (m¹G37)-methyltransferases that catalyzes the identical tRNA modification, m¹G37 (36, 37). To further examine if the m.4435A→G mutation introduced the m¹G37 modification of tRNA^{Met}, we prepared wildtype and mutant tRNAs by *in vitro* transcription and evaluated the methylation activity catalyzed by the recombinant *M. jannaschii* Trm5 (*Mj-Trm5*) (36, 37). As shown in Fig. 2A, the mutant tRNA^{Met} transcripts (G37) were modified with m¹G37 modification by the *Mj-Trm5* but as less efficiently as cytoplasmic tRNA^{Leu(CAG)} transcripts (G37) (10). In contrast, the modification was not detected in the wildtype tRNA^{Met} transcripts (A37) in the presence of *Mj-Trm5*. As controls, the human cytoplasmic tRNA^{Leu(CAG)} transcripts (G37) were modified by the *Mj-Trm5*, whereas human cytoplasmic tRNA^{Thr} transcripts (A37) were not modified in the presence of *Mj-Trm5*. These results indicated that the substitution of A to G at position 37 introduced the m¹G37 modification of tRNA^{Met}.

We then analyzed the binding affinities of tRNA^{Met} with *Mj-Trm5* using an electrophoretic mobility shift assay. The shift representing the Trm5–tRNA complex occurred at an enzyme concentration of 0.25 μ M. As shown in Fig. 2B, the mutant

³ The abbreviations used are: ROS, reactive oxygen species; DIG, digoxigenin; OCR, oxygen consumption rate; FCCP, carbonyl cyanide *p*-trifluoromethoxyphenylhydrazone; $\Delta\Psi_m$, mitochondrial membrane potentials.

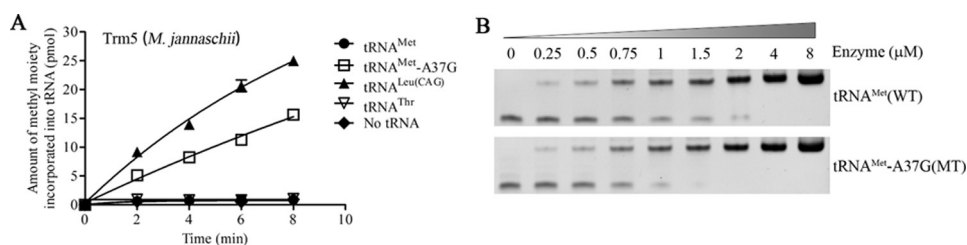


Figure 2. Methylation activity assays. The unmodified human mitochondrial wildtype (A37) and mutant (G37) $tRNA^{Met}$, cytosolic $tRNA^{Leu(CAG)}$, and $tRNA^{Thr}$ were generated from *in vitro* transcription. **A**, analysis for the m^1G37 modification of $tRNA^{Met}$. The unmodified tRNA transcripts were incubated with *M. jannaschii* (*Mj*-Trm5) in the presence of *S*-adenosyl-L-methionine. Samples were withdrawn and stopped after 2, 4, 6, or 8 min, respectively. The relative modification efficiency was calculated from the initial phase of the reaction. The calculations were based on three independent determinations. Graph shows the results of a representative experiment. **B**, electrophoretic mobility shift assay. The unmodified mitochondrial wildtype (A37) and mutant (G37) $tRNA^{Met}$ were incubated with various concentrations of enzymes *Mj*-Trm5. These samples were electrophoresed through 6% polyacrylamide gel and stained with ethidium bromide.

and wildtype $tRNA^{Met}$ transcripts were fully shifted to the *Mj*-Trm5- $tRNA$ complex at enzyme concentrations of 1.5 and 4.0 μM , with the calculated K_d value of 1.105 ± 0.028 and $1.822 \pm 0.025 \mu M$, respectively. These data provided further evidence that the m.4435A→G mutation introduced the m^1G37 modification of $tRNA^{Met}$.

Altered conformation and stability of $tRNA^{Met}$

It was anticipated that the m.44535A→G mutation caused structural alteration and the instability of $tRNA^{Met}$. To test if the m.4435A→G mutation affected the conformation of $tRNA^{Met}$, total RNAs from mitochondria isolated from mutant and control cell lines were electrophoresed through a 10% native gel and then electroblotted onto a positively charged nylon membrane for hybridization analysis with oligodeoxynucleotide probes for $tRNA^{Met}$ and $tRNA^{Thr}$, $tRNA^{Leu(CUN)}$ and $tRNA^{Ser(AGY)}$, respectively. As shown in Fig. 3A, electrophoretic patterns showed that the $tRNA^{Met}$ in three mutant cybrid cell lines carrying the m.4435A→G mutation migrated faster than those of control cybrid cell lines lacking this mutation.

We then examined the stability of the wildtype and mutant $tRNA^{Met}$ transcripts through the measurement of the melting temperatures (T_m) by calculating the derivatives of the absorbance against a temperature curve. As shown in Fig. 3B, the T_m values for wildtype (A37) and mutant (G37) transcripts were 43.52 ± 0.71 and 46.02 ± 0.41 °C, respectively. These results suggested that the m.4435A→G mutation affected the stability of $tRNA^{Met}$.

Marked decrease in the steady-state levels of $tRNA^{Met}$

To assess if the m.4435A→G mutation ablated the metabolism of $tRNA^{Met}$, we subjected mitochondrial RNAs from mutant and control cybrid cell lines to Northern blots and hybridized them with DIG-labeled oligodeoxynucleotide probes for $tRNA^{Met}$, $tRNA^{Lys}$, $tRNA^{Thr}$, and $tRNA^{Leu(CUN)}$ derived from the heavy (H)-strand transcription unit and $tRNA^{Ser(UCN)}$ and $tRNA^{Glu}$ derived from the light (L)-strand transcription unit (38, 39). As shown in Fig. 4A, the steady-state level of $tRNA^{Met}$ in the mutant cells was markedly decreased compared with those in control cells. For comparison, the average levels of $tRNA^{Met}$ in the mutant cybrid cell lines were among ~74.4, 69.5, 73.3, 64.9, and 75.3% of average values of three control cybrids after normalization to $tRNA^{Lys}$, $tRNA^{Thr}$,

$tRNA^{Leu(CUN)}$, $tRNA^{Ser(UCN)}$, and $tRNA^{Glu}$ ($p = 0.0001$ to 0.0003), respectively.

Deficient aminoacylation of $tRNA^{Met}$

To evaluate if the m.4435A→G mutation affects aminoacylation of $tRNA$, we examined the aminoacylation level of $tRNA^{Met}$ as well as $tRNA^{Leu(UUR)}$, $tRNA^{Leu(CUN)}$, $tRNA^{Ile}$, and $tRNA^{His}$ by the use of electrophoresis in an acidic urea PAGE system to separate uncharged $tRNA$ species from the corresponding charged $tRNA$, electroblotting and hybridizing with the $tRNA$ probes described above. As shown in Fig. 5A, the upper band represents the charged $tRNA$, and the lower band represents uncharged $tRNA$. There were no obvious differences in electrophoretic mobility between the control and mutant cell lines. To further distinguish nonaminoacylated $tRNA$ from aminoacylated $tRNA$, samples of $tRNAs$ were deacylated by being heated for 10 min at 60 °C (pH 8.3) and then run in parallel. As shown in Fig. 5B, only one band (uncharged $tRNA$) was present in both mutant and control cell lines after deacylating. However, the efficiencies of aminoacylated $tRNA^{Met}$ in the mutant cell lines varied from 61.6 to 83.2%, with the average of 69%, relative to the average values of control cell lines ($p = 0.034$) (Fig. 5C). However, the levels of aminoacylation in $tRNA^{Leu(UUR)}$, $tRNA^{Leu(CUN)}$, $tRNA^{Ile}$, and $tRNA^{His}$ in mutant cell lines were comparable with those in the control cell lines.

Decreases in the levels of mitochondrial proteins

To investigate whether the aberrant $tRNA$ metabolism caused by the m.4435A→G mutation impaired mitochondrial translation, a Western blot analysis was carried out to examine the steady-state levels of seven oxidative phosphorylation subunits of (encoded by mtDNA) in mutant (5) and control cell lines, whereas Tom20 (encoded by nuclear gene) as a loading control. As shown in Fig. 6A, the overall levels of seven mitochondrial translation products in the mutant cell lines ranged from ~29.6 to 97.5%, with an average of 67.2% ($p < 0.0001$), relative to the mean value measured in the control cell lines. However, there were variable reductions in levels of ND3, ND4, and ND5, subunits 3, 4, and 5 of NADH dehydrogenase; ATP6, ATP8, subunits 6 and 8 of the H^+ -ATPase; CYTB, apocytochrome *b*; CO₂, subunit II of cytochrome *c* oxidase in mutant cell lines. In particular, mutant cell lines exhibited marked reductions (49.4 to 70.4%) in the levels of ND3, ATP6, and CYTB harboring 3.9 to 7.0% methionine codons, whereas rela-

Hypertension-linked mitochondrial tRNA^{Met} mutation

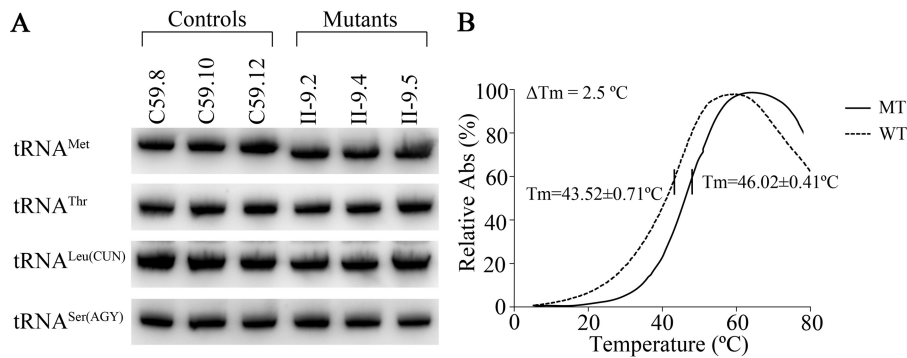


Figure 3. The analysis of the stability of tRNA^{Met}. A, Northern blot analysis of tRNA under native conditions. Two μg of total mitochondrial RNA from various cell lines were electrophoresed through native polyacrylamide gels, electroblotted, and hybridized with DIG-labeled oligonucleotide probes specific for the tRNA^{Met}, tRNA^{Thr}, tRNA^{Leu(CUN)}, and tRNA^{Ser(AGY)}, respectively. B, thermal stability of wildtype (A37) and mutant (G37) tRNA^{Met}. ΔT_m indicates the difference of the T_m value between wildtype (A37) and mutant (G37) tRNA^{Met}. The calculations were based on three independent experiments.

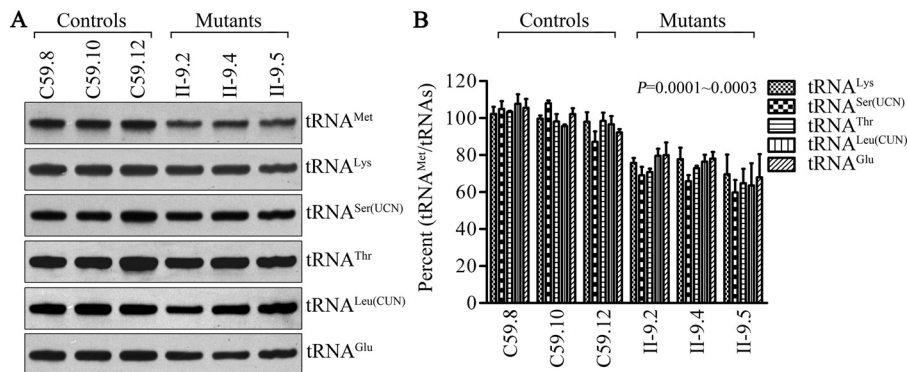


Figure 4. Northern blot analysis of tRNA under a denaturing condition. A, $2 \mu\text{g}$ of total mitochondrial RNA from various cell lines were electrophoresed through a denaturing polyacrylamide gel, electroblotted, and hybridized with DIG-labeled oligonucleotide probes specific for the tRNA^{Met}, tRNA^{Lys}, tRNA^{Ser(UCN)}, tRNA^{Thr}, tRNA^{Leu(CUN)}, and tRNA^{Glu}, respectively. B, quantification of tRNA levels. Average relative tRNA^{Met} content per cell, normalized to the average content per cell of tRNA^{Lys}, tRNA^{Ser(UCN)}, tRNA^{Thr}, tRNA^{Leu(CUN)}, and tRNA^{Glu} in three cybrid cell lines derived from one affected subject (II-9) and three cybrid cell lines derived from one Chinese control subject (C59). The values for the latter are expressed as percentages of the average values for the control cell lines. The calculations were based on three independent experiments. The error bars indicate mean \pm 2 S.D. P indicates the significance, according to the *t* test, of the differences between mutant and control cell lines.

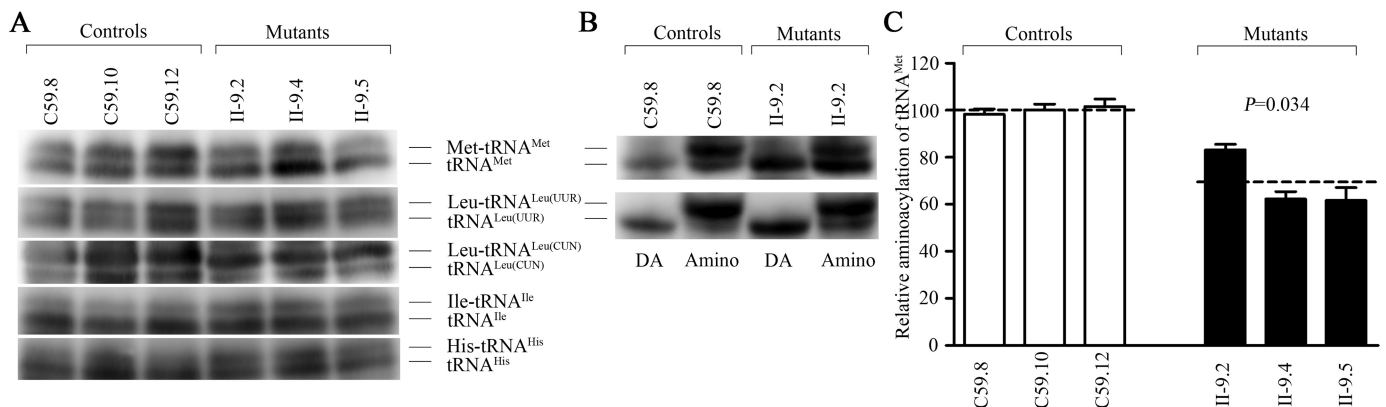


Figure 5. *In vivo* aminoacylation assays. A, $2 \mu\text{g}$ of total mitochondrial RNA purified from six cell lines under acid conditions were electrophoresed at 4°C through an acid (pH 4.5) 10% polyacrylamide, 8 M urea gel, electroblotted, and hybridized with DIG-labeled oligonucleotide probes specific for the tRNA^{Met}, tRNA^{Leu(UUR)}, tRNA^{Leu(CUN)}, tRNA^{Ile}, and tRNA^{His}, respectively. B, the samples from one control (C59-8) and one mutant (II-9.2) cell lines were deacylated (DA) by heating for 10 min at 60°C (pH 8.3), electrophoresed, and hybridized with DIG-labeled oligonucleotide probes specific for tRNA^{Met} and tRNA^{Leu(UUR)}. C, quantification of aminoacylated proportions of tRNA^{Met} in the mutant and controls. The calculations were based on three independent experiments. Graph details and symbols are explained in the legend to Fig. 4.

tively mild reductions (2.5 to 22.9%) of the levels of ND4, ND5, ATP8, and CO₂ containing 4.3 to 8.7% methionine codons were observed in mutant cell lines. However, the levels of polypeptide synthesis in mutant cells, relative to those in control cells, showed no significant correlation with either the number of codons or the proportion of methionine (Table S1).

Reduced activities of respiratory chain complexes I, III, IV, and V

To evaluate the effect of the m.4435A→G mutation on the oxidative phosphorylation, we measured the activities of respiratory complexes by the use of isolating mitochondria from

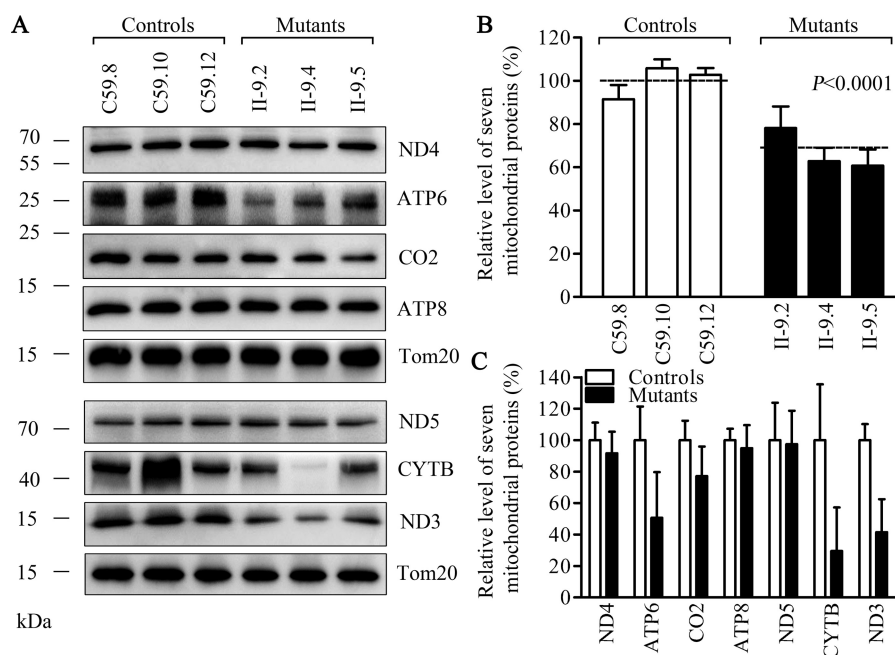


Figure 6. Western blot analysis of mitochondrial proteins. A, 20 μ g of total cellular proteins from various cell lines were electrophoresed through a denaturing polyacrylamide gel, electroblotted, and hybridized with 7 polypeptides (mtDNA-encoded subunits of respiratory complexes) and with Tom20 as a loading control. B, quantification of total mitochondrial protein levels. The levels of mitochondrial proteins in 3 mutant cell lines and 3 control cell lines were determined as described elsewhere (53, 54). C, quantification of 7 polypeptides. The levels of ND3, ND4, ND5, CO₂, CYTB, ATP6, and ATP8 in three mutant cell lines and three control cell lines were determined as described elsewhere (53, 54). Graph details and symbols are explained in the legend to Fig. 4.

three mutant and three control cell lines. The activity of Complex I (NADH ubiquinone oxidoreductase) was determined through the oxidation of NADH with ubiquinone as the electron acceptor (40–42). Complex II (succinate ubiquinone oxidoreductase) was the only respiratory complex that was encoded by the nuclear DNA, so we examined the activity of complex II through the artificial electron acceptor dichlorophenolindophenol (41, 42). The activity of complex III (ubiquinone cytochrome *c* oxidoreductase) was measured through the reduction of cytochrome *c* (III) by using D-ubiquinol-2 as the electron donor. The activity of complex IV (cytochrome *c* oxidase) was monitored through the oxidation of cytochrome *c* (II). The activity of complex V (F₁-ATP synthase) was explored through the NADH oxidation via conversion of phosphoenolpyruvate to lactate by a two-step reaction (41). As shown in Fig. 7, the activity of complexes I, III, IV, and V in the mutant cells carrying the m.4435A→G mutation were 78.8 ($p = 0.013$), 71.6 ($p < 0.001$), 81.1 ($p = 0.003$), and 73.0% ($p = 0.018$) of the mean value measured in three control cell lines, respectively, whereas the activity of complex II in the mutant cells carrying the m.4435A→G mutation was 99.5% of the mean value measured in three control cell lines ($p = 0.868$), which was similar to the activity of complex II in the wildtype cell lines as expected.

Respiration deficiency

To evaluate if the m.4435A→G mutation alters cellular bioenergetics, we examined the oxygen consumption rates (OCR) of three mutant cell lines carrying the m.4435A→G mutation and three control cell lines (43). As shown in Fig. 8, the basal OCR in mutant cell lines was 57.8% ($p < 0.001$) relative to the mean value measured in the control cell lines. To investigate

which of the enzyme complexes of the respiratory chain were affected in the mutant cell lines, oligomycin (to inhibit the ATP synthase), carbonyl cyanide *p*-trifluoromethoxyphenylhydrazone (FCCP) (to uncouple the mitochondrial inner membrane and allow for maximum electron flux through the ETC), rotenone (to inhibit complex I), and antimycin A (to inhibit complex III) were added sequentially while measuring OCR. The difference between the basal OCR and the drug-insensitive OCR yields the amount of ATP-linked OCR, proton leak OCR, maximal OCR, reserve capacity, and non-mitochondrial OCR. As shown in Fig. 8, the ATP-linked OCR, proton leak OCR, maximal OCR, reserve capacity, and non-mitochondrial OCR in mutant cell lines were ~53.1 ($p < 0.001$), 79.7 ($p = 0.122$), 48.6 ($p < 0.001$), 40.1 ($p < 0.001$), and 99.5% ($p = 0.880$), relative to the mean value measured in the control cell lines, respectively.

Reduced level in mitochondrial ATP production

We used the luciferin/luciferase assay to examine the capacity of oxidative phosphorylation in mutant and wildtype cell lines. Populations of cells were incubated in the media in the presence of glucose, and 2-deoxy-D-glucose with pyruvate (44). As shown in Fig. 9A, the levels of ATP production in mutant cell lines in the presence of glucose (total cellular levels of ATP) were comparable with those measured in control cell lines. In contrast, as shown in Fig. 9B, the levels of ATP production in mutant cell lines, in the presence of 2-deoxy-D-glucose and pyruvate to inhibit the glycolysis (mitochondrial levels of ATP), varied from 66.0 to 73.1%, with an average of 69.8% relative to the mean value measured in the control cell lines ($p < 0.001$).

Hypertension-linked mitochondrial tRNA^{Met} mutation

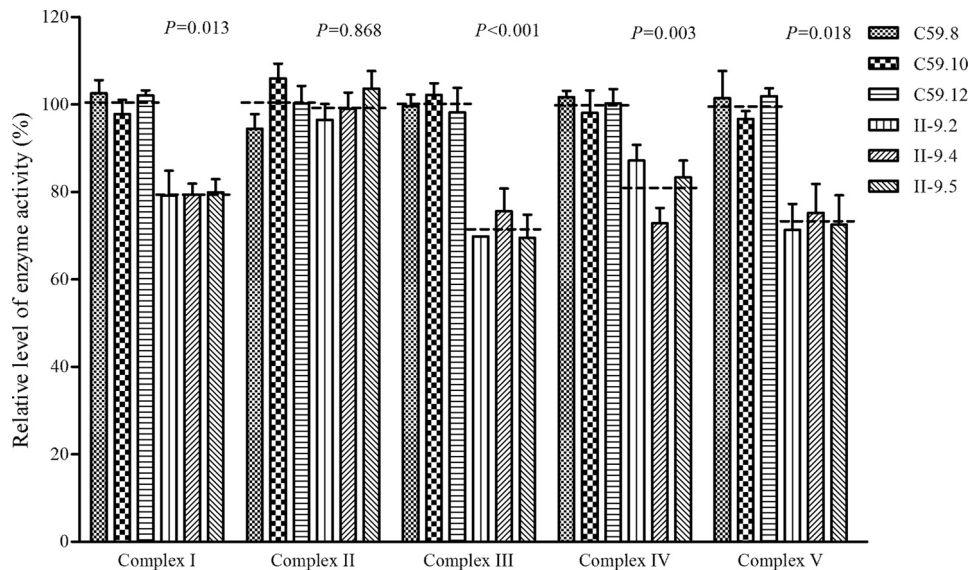


Figure 7. Enzymatic activities of respiratory chain complexes. The activities of respiratory complexes were investigated by enzymatic assay on complexes I, II, III, IV, and V in mitochondria isolated from various cell lines. The calculations were based on 4 independent experiments. Graph details and symbols are explained in the legend to Fig. 4.

Decrease in mitochondrial membrane potential

The mitochondrial membrane potentials ($\Delta\Psi_m$) were measured through the fluorescence probe JC-10 assay system in three mutant and three control cell lines (45). The ratio of fluorescence intensities excitation/emission = 490/590 and 490/530 nm (FL590/FL530) were recorded to delineate the $\Delta\Psi_m$ of each sample. The relative ratios of FL590/FL530 geometric mean between mutant and control cell lines were calculated to represent the level of $\Delta\Psi_m$, as described elsewhere (44). As shown in Fig. 10, the $\Delta\Psi_m$ of three mutant cell lines carrying the m.4435A→G mutation ranged from 62.8 to 64.0%, with an average 63.4% ($p < 0.001$) of the mean value measured in three control cell lines. In contrast, the levels of $\Delta\Psi_m$ in mutant cell lines in the presence of FCCP were comparable with those of control cell lines ($p = 0.290$).

The increase of ROS production

The levels of mitochondrial ROS among the cybrids derived from three mutant cybrid cell lines carrying the m.4435A→G mutation and three control cybrid cell lines lacking the mutation were determined using MitoSOX assay via flow cytometry under normal conditions and then following H₂O₂ stimulation (46–48). Geometric mean intensity was recorded to measure the production rate of ROS of each sample. As shown in Fig. 11, A and B, the levels of ROS generation in the mutant cell lines carrying the m.4435A→G mutation ranged from 140.0 to 157.4%, with an average 147.5% ($p < 0.001$) of the mean value measured in three control cell lines under unstimulated conditions. As illustrated in Fig. 11, C and D, the levels of ROS generation in the mutant cell lines varied from 157.1 to 170.9%, with an average 165.6% ($p < 0.001$) of the mean value measured in the control cell lines under stimulation conditions.

Discussion

In the present study, we investigated the pathogenic mechanism of the hypertension-associated m.4435A→G mutation in

the tRNA^{Met} gene. The occurrences of the m.4435A→G mutation in four genetically unrelated Chinese families affected by hypertension strongly indicate that this mutation is involved in the pathogenesis of this disease (31–33). The m.4435A→G mutation affected a highly conserved adenosine (A37), adjacent to the 3' end of the anticodon of tRNA^{Met} (3, 7). The nucleotides at position 37 (A or G) of tRNAs are often modified, by such processes as thiolation and methylthiolation (3, 15). However, nucleotides at this position in 5 of 22 mammalian mitochondrial tRNAs including tRNA^{Met} and tRNA^{ASP} were not modified (9, 28). In particular, neither i⁶A37 nor t⁶A37 modification was detected in the mammalian mitochondrial tRNA^{Met} (9). Therefore, it was hypothesized that the substitution of A37 with G37 caused by the m.4435A→G mutation created the m¹G37 modification of tRNA^{Met}, catalyzed by TRMT5. *In vitro* assays showed that the m.4435A→G mutation impaired the f5C formation mediated by NSUN3 (49). In this study, the primer extension experiment revealed that the m.4435A→G mutation introduced the m¹G37 modification of tRNA^{Met}. This hypothesis was further supported by the fact that an archaea *M. jannaschii* Trm5 catalyzed the m¹G37 modification in the unmodified mutant (G37) but not wildtype (A37) tRNA^{Met} transcripts. Furthermore, an electrophoretic mobility shift assay showed that *M. jannaschii* Trm5 had higher affinity with the mutant tRNA^{Met} transcripts (G37) than the wildtype tRNA^{Met} transcript (A37). These data demonstrated that the m.4435A→G mutation created the m¹G37 modification of tRNA^{Met}, catalyzed by TRMT5.

Modification at position 37 contributes to the high fidelity of codon recognition and the structural formation and stabilization of functional tRNAs (3, 15, 50, 51). In *Escherichia coli*, the deficient modification of A37 decreased the activity of the corresponding tRNA (52) and increased +1 frameshifts for tRNA^{Phe} (53), whereas the A to G substitution at position 37 led to a 10-fold reduction in the section of tRNAs at the A-site (54). Therefore, the m¹G37 modification introduced

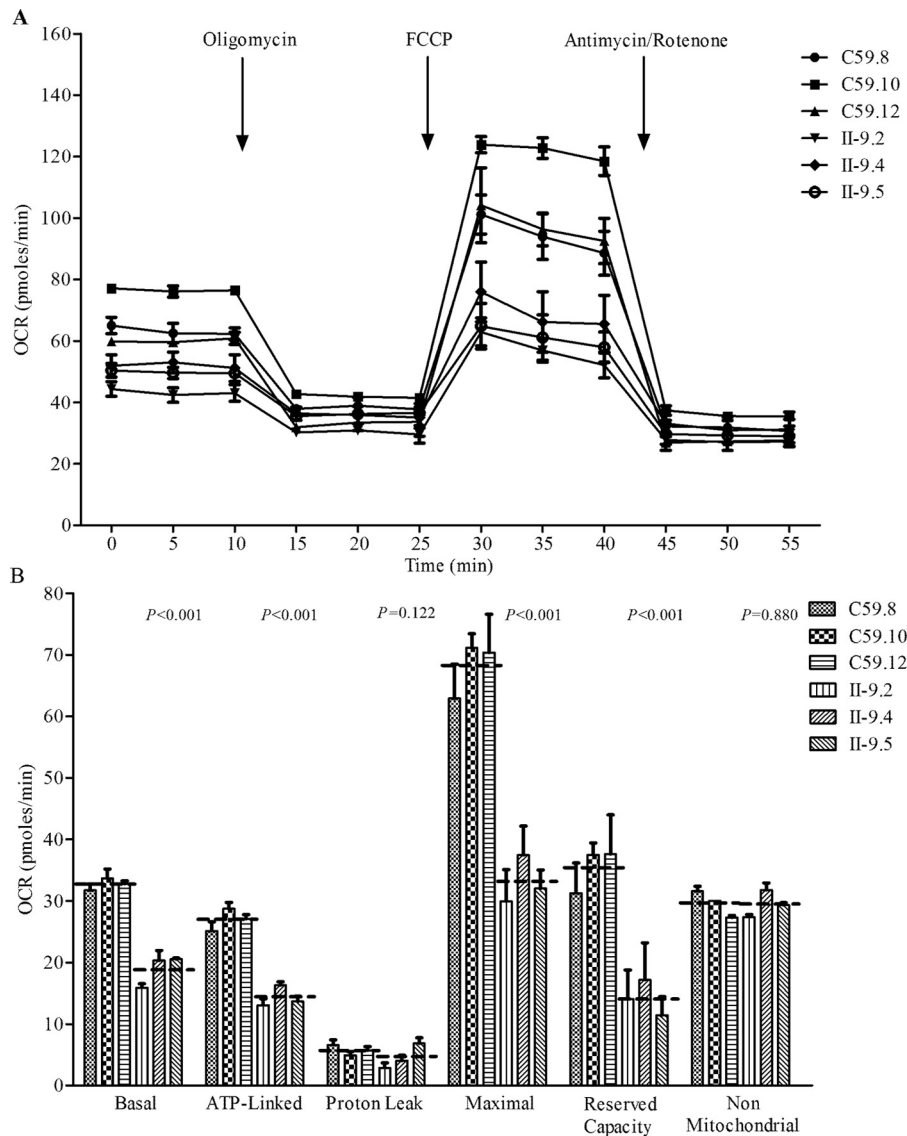


Figure 8. Respiration assays. *A*, an analysis of O_2 consumption in the various cell lines using different inhibitors. The rates of O_2 (OCR) were first measured on 2×10^4 cells of each cell line under basal conditions and then sequentially added to oligomycin ($1.5 \mu M$), FCCP ($0.5 \mu M$), rotenone ($1.0 \mu M$), and antimycin A ($1.0 \mu M$) at the indicated times to determine different parameters of mitochondrial functions. *B*, graphs presented the ATP-linked OCR, proton leak OCR, maximal OCR, reserve capacity, and non-mitochondrial OCR in mutant and control cell lines. Non-mitochondrial OCR was determined as the OCR after rotenone/antimycin A treatment. Basal OCR was determined as OCR before oligomycin minus OCR after rotenone/antimycin A. ATP-linked OCR was determined as OCR before oligomycin minus OCR after oligomycin. Proton leak was determined as basal OCR minus ATP-linked OCR. Maximal was determined as the OCR after FCCP minus non-mitochondrial OCR. Reserve Capacity was defined as the difference between Maximal OCR after FCCP minus Basal OCR. The average values of 3–5 independent experiments for each cell line are shown, the horizontal dashed lines represent the average value for each group. Graph details and symbols are explained in the legend to Fig. 4.

by the m.4435A→G mutation altered the structure and function of $tRNA^{Met}$, as in the case of m.7551A→G mutation in the $tRNA^{Asp}$ (28). Here, the altered structure of $tRNA^{Met}$ caused by the m.4435A→G mutation was evidenced by the increased melting temperature and electrophoretic mobility of mutated $tRNA$ with respect to the wildtype molecule. Furthermore, the m.4435A→G mutation caused 31% reduction in aminoacylated efficiency of $tRNA^{Met}$ in mutant cell lines, in contrast to the increasing efficiency of aminoacylation in several $tRNAs$ caused by TRMU mutation (22). Both altered structure and improper aminoacylation of $tRNA^{Met}$ made the mutant $tRNA^{Met}$ to be metabolically less stable and more subject to degradation, thereby lowering the level of this $tRNA$, as in the case of $tRNA^{Asp}$ 7551A→G mutation (28). In the present study,

40% reductions in the steady-state level of $tRNA^{Met}$ observed in mutant cell lines were consistent with the previous observations in the lymphoblastoid cell lines bearing the m.4435A→G mutation (30, 31). However, the reduced levels of $tRNA^{Met}$ in mutant cells harboring the m.4435A→G mutation were indeed above the proposed threshold, which is 30% of the control levels of $tRNA$, to support the normal rate of mitochondrial translation (39, 44, 55, 56), indicating that the m.4435A→G mutation itself is insufficient to produce a clinical phenotype.

The inefficient aminoacylation and shortage of $tRNA^{Met}$, or the faulty interaction between mutant $tRNA^{Met}$ and the translational machinery, contributed to the defective mitochondrial translation (57, 58). In the present study, reduced levels of mitochondrial proteins (an average decrease of ~33%) were compa-

Hypertension-linked mitochondrial tRNA^{Met} mutation

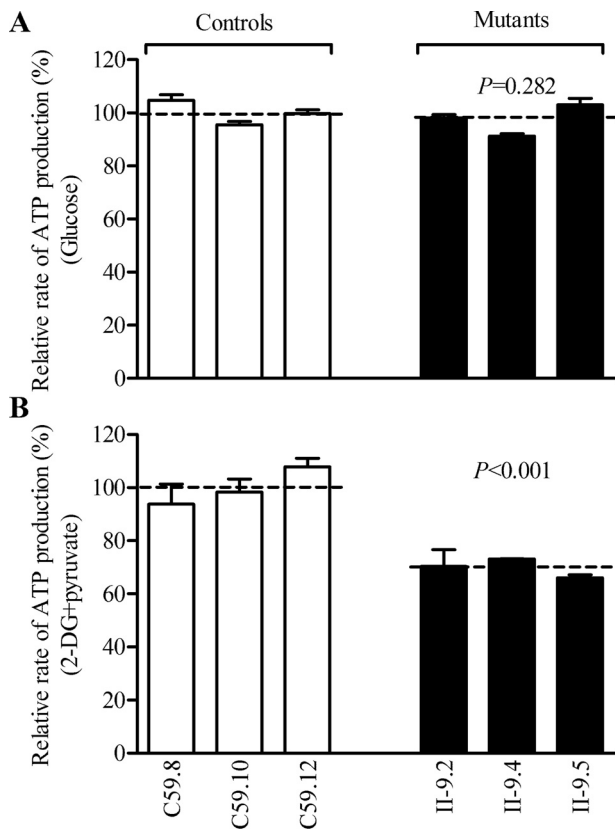


Figure 9. Measurement of cellular and mitochondrial ATP levels using bioluminescence assay. Cells were incubated with 10 mM glucose or 5 mM 2-deoxy-D-glucose plus 5 mM pyruvate to determine ATP generation under mitochondrial ATP synthesis. Average rates of ATP level per cell line and are shown: A, ATP level in total cells. B, ATP level in mitochondria. Three independent experiments were made for each cell line. Graph details and symbols are explained in the legend to Fig. 4.

rable with the reduced rate of mitochondrial translation observed in cell lines carrying the tRNA^{Asp} 7551A→G, tRNA^{Ile} 4263A→G, tRNA^{Glu} 14692A→G, and tRNA^{Ala} 5655A→G mutations (4, 28, 35, 56). The variable decreases in the levels of 7 mtDNA-encoded polypeptides were observed in the mutant cell lines. As shown in Table S2, mutant cell lines carrying the m.4435A→G mutation exhibited marked reductions (49.4 to 70.4%) in the levels of 3 polypeptides (ND3, ATP6, and CYTB), and relative mild reductions (2.5 to 23%) in the levels of ND4, ND5, CO₂, and ATP8. In contrast to what was previously shown in cells carrying the tRNA^{Lys} 8344A→G and tRNA^{Ser}-(UCN) 7445A→G mutations (39, 58), the reduced levels of these polypeptides in mutant cell lines did not significantly correlate with the number or proportion of methionine codons. The impaired synthesis of these polypeptides was responsible for the reduced activities of complexes I, III, IV, and complex V. Furthermore, the impairment of mitochondrial translation resulted in the reduced rates in the basal OCR, or ATP-linked OCR, reserve capacity, and maximal OCR in the mutant cell lines. These observations highlighted an important role of tRNA^{Met} metabolic failure in producing their respiratory phenotypes, as in the cases of cell lines harboring the tRNA^{Asp} 7551A→G and tRNA^{Glu} 14692T→C mutations (4, 28).

The respiratory deficiency caused by the m.4435A→G mutation may cause uncoupling of the oxidative pathway for

ATP synthesis, oxidative stress, and subsequent failure of the cellular energetic process (59). In this investigation, 32% decreases in mitochondrial ATP production in the cell lines carrying the m.4435A→G mutation, which may be caused by the defective activity of complexes I, III, IV, and V, was comparable with those in cell lines carrying the tRNA^{Glu} 14692T→C, tRNA^{Asp} 7551A→G, and tRNA^{Ala} 5655A→G mutations (4, 28, 35). Furthermore, the deficient oxidative phosphorylation often affected mitochondrial membrane potentials, which reflect the pumping of hydrogen ions across the inner membrane during the process of electron transport and oxidative phosphorylation (44, 46). In this study, 37% reduction in mitochondrial membrane potential in cybrid cell lines carrying the m.4435A→G mutation was comparable with those in cell lines carrying the tRNA^{Glu} 14692T→C and tRNA^{Asp} 7551A→G (4, 28). The abnormal oxidative phosphorylation and mitochondrial membrane potential enhanced the production of reactive oxygen species and the subsequent failure of cellular energetic processes in mutant cells carrying the m.4435A→G mutation. In particular, the overproduction of ROS can establish a vicious cycle of oxidative stress in the mitochondria, thereby damaging mitochondrial and cellular proteins, lipids, and nucleic acids and increasing apoptotic signaling (60, 61). The skeletal and vascular smooth muscles may be preferentially involved because they were exquisitely sensitive to inefficient metabolism, subtle imbalance in cellular redox state, and increased level of free radicals (62, 63). An inefficient metabolism caused by the mitochondrial dysfunction in skeletal and vascular smooth muscles may lead to the elevation of systolic blood pressure and therefore be involved in hypertension. The relative mild mitochondrial dysfunction caused by the m.4435A→G mutation suggested that the mutation is an inherited risk factor necessary for the development of hypertension but may by itself be insufficient to produce a clinical phenotype. The nuclear genetic or epigenetic factors and lifestyles may contribute to the development of clinical phenotypes in subjects bearing the m.4435A→G mutation (64, 65). In particular, the tissue-specific effect of this tRNA mutation may be attributed to the tissue-specific RNA metabolism or the involvement of nuclear modifier genes (66–69).

In summary, our findings suggested the pathogenic mechanism leading to an impaired oxidative phosphorylation in cells carrying the hypertension-associated m.4435A→G mutation in the tRNA^{Met} gene. The m.4435A→G mutation altered the structure and function of tRNA^{Met}. The aberrant tRNA metabolism resulted in the defects in mitochondrial translation, respiratory deficiency, decreasing membrane potentials and ATP production, and finally increasing ROS production. As a result, mitochondrial dysfunction caused by the m.4435A→G mutation manifests hypertension. However, the tissue specificity of this pathogenic mtDNA mutation is likely due to the involvement of nuclear modifier genes or tissue-specific differences in tRNA metabolism. Thus, our findings may provide new insights into the pathophysiology of hypertension, which was manifested by the deficient modification of mitochondrial tRNA^{Met}.

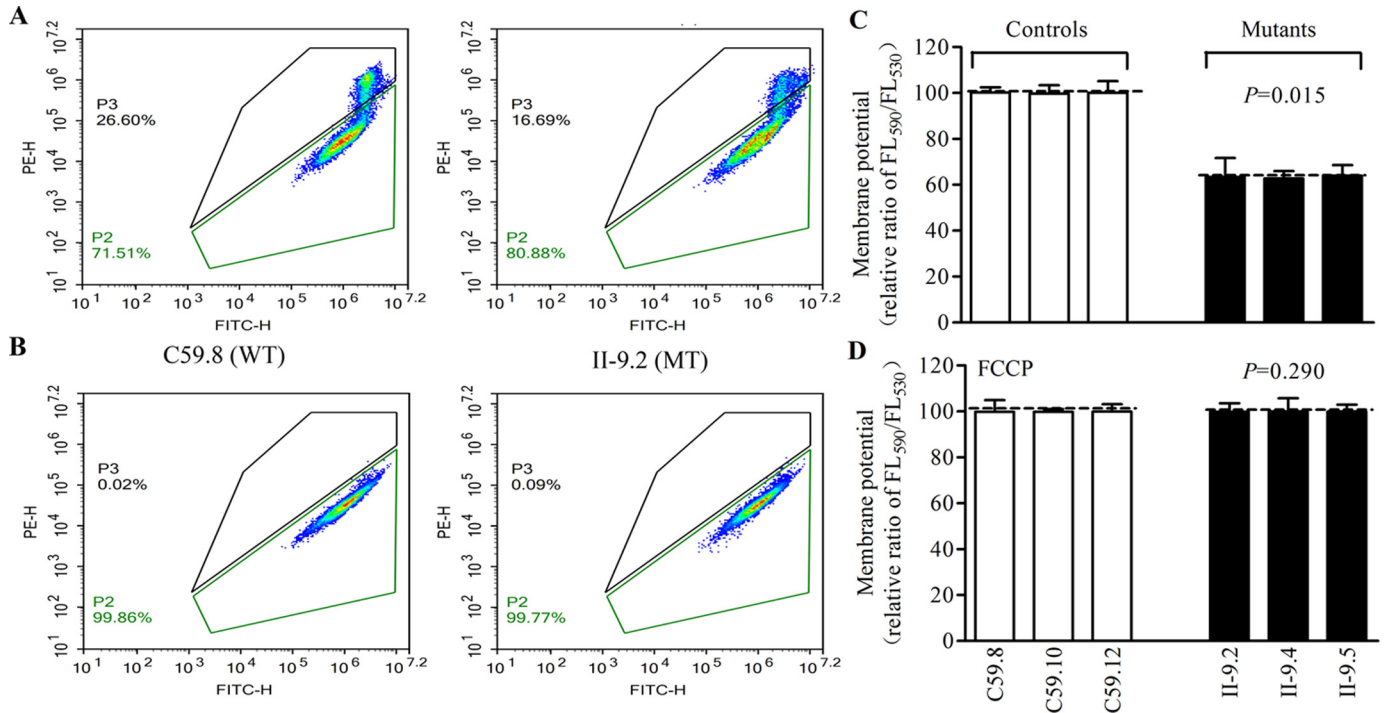


Figure 10. Mitochondrial membrane potential analysis. $\Delta\Psi_m$ was measured in three mutant and three control cell lines using a fluorescence probe JC-10 assay system. The ratio of fluorescence intensities excitation/emission = 490/590 and 490/530 nm (FL₅₉₀/FL₅₃₀) were recorded to delineate the $\Delta\Psi_m$ level of each sample. Represented flow cytometry images of cell lines II-9.2 and C59.8 with (A) and without (B) 10 μ M FCCP. Relative ratio of JC-10 fluorescence intensities at excitation/emission = 490/530 and 490/590 nm in the absence (C) and presence (D) of 10 μ M FCCP. The average of three to five determinations for each cell line are shown. Graph details and symbols are explained in the legend to Fig. 4.

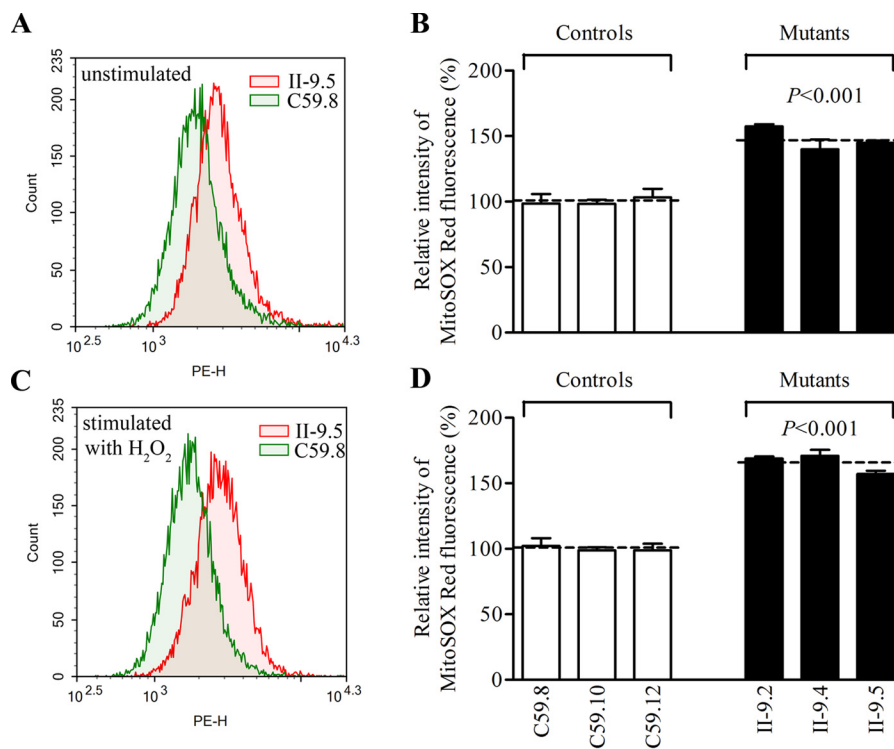


Figure 11. Measurement of ROS. Ratio of geometric mean intensity between levels of the ROS generation in the vital cells with or without H₂O₂ stimulation. The rates of production in ROS from three mutant cell lines and three control cell lines were analyzed by BD-LSR II flow cytometer system using MitoSox (5 μ M) either without (A) or with (C) H₂O₂ stimulation. The relative ratio of intensity (stimulated or unstimulated with H₂O₂) was calculated. B and D, the average of three independent determinations for each cell lines is shown. Graph details and symbols are explained in the legend to Fig. 4.

Hypertension-linked mitochondrial tRNA^{Met} mutation

Experimental procedures

Cell lines and culture conditions

Immortalized lymphoblastoid cell lines were generated from one hypertensive matrilineal relative (II-9) of a Chinese family carrying the m.4435A→G mutation (33) and one genetically unrelated Chinese control individual (C59) belonging to the same mtDNA haplogroup B5 but lacking the mutation (Table S2) (70). These cell lines were grown in RPMI 1640 medium with 10% fetal bovine serum (FBS). The bromodeoxyuridine (BrdU)-resistant 143B.TK⁻ cell line was grown in Dulbecco's modified Eagle's medium (DMEM) (Life Technologies) (containing 4.5 mg of glucose and 0.11 mg of pyruvate/ml), supplemented with 100 μg of BrdU/ml and 5% FBS. The mtDNA-less ρ⁰206 cell line, derived from 143B.TK⁻ (34, 35, 71) was grown under the same conditions as the parental line, except for the addition of 50 μg of uridine/ml. Transformation by cytoplasts of mtDNA-less ρ⁰206 cells using one affected subject (II-9) carrying the m.4435A→G mutation and one control individual (C59) was performed as described elsewhere (34, 35, 71). All cybrid cell lines constructed with enucleated lymphoblastoid cell lines were maintained in the same medium as the 143B.TK⁻ cell line. An analysis for the presence and level of the m.4435A→G mutation was carried out as described previously (Fig. S1) (31). Quantification of the mtDNA copy number from different cybrids was performed as detailed elsewhere (47). Three mutant cybrids (II-9.2, II-9.4, and II-9.5) carrying the m.4435A→G mutation and three control cybrids (C59.8, C59.10, and C59.12) lacking the mutation with similar mtDNA copy numbers and the same karyotype were used for the biochemical characterization described below.

Primer extension assay

A primer extension experiment to analyze the m¹G37 modification of tRNA^{Met} was carried out by a modified procedure, as described elsewhere (72, 73). Total mitochondrial RNAs were obtained from mitochondria isolated from mutant and control cell lines (~2.0 × 10⁸ cells) using the TOTALLY RNATM kit (Ambion), as described previously (74). A DNA primer (5'-TGGTAGTACGGGAAGGGTATAACCAACATT-3') complementary to the 3' end of the tRNA^{Met} was 5' end labeled with DIG. Two μg of total mitochondrial RNA as templates and 1 μM DIG-labeled oligodeoxynucleotide probe specific for the tRNA^{Met} were used in the PrimeScript II 1st Strand cDNA Synthesis Kit (TAKARA) for reverse transcription. Extension reactions were carried out as detailed previously (72, 73). The samples were applied onto 15% PAGE with 8 M urea in Tris borate-EDTA buffer and electroblotted onto a positively charged nylon membrane (Roche).

Methylation activity assays

The fragments spanning tRNA^{Met} (corresponding to mtDNA at positions 4402–4469) were PCR-amplified genomic DNAs from one hypertensive subject (II-9) carrying the m.4435A→G mutation and control subject (C59) and cloned into the HindIII/BamHI sites of pUC19. The plasmid carrying the human cytoplasmic tRNA^{Leu(CAG)} and tRNA^{Thr} genes were the gifts from Dr. En-Duo Wang (75, 76). The unmodified

tRNAs were generated by *in vitro* transcription using T7 RNA polymerase, as detailed elsewhere (77). The purifications of archaeal Trm5 (aTrm5) from *M. jannaschii* (Mj-Trm5) was performed as detailed previously (36, 37). The methylation reaction contained 200 μM [³H]SAM, 50 mM Tris-HCl (pH 7.0), 100 mM KCl, 10 mM MgCl₂, 100 μg/ml of bovine serum albumin (BSA), 5 mM DTT, and 5 μM transcribed wildtype or mutant tRNA^{Met}. The reaction was initiated by the addition of 2 μM Mj-Trm5. Reactions were performed under identical conditions at 37 °C, at time intervals ranging between 2 and 8 min, aliquots of 5 μl were removed, absorbed on paper discs, and precipitated in trichloroacetic acid.

Electrophoretic mobility shift assay

Electrophoretic mobility shift assay (EMSA) was performed as described elsewhere (78, 79). A range of 0.25–8 μM Mj-Trm5 was incubated with 100 nM tRNA in the presence of a 30-μl reaction volume including 50 mM Tris-HCl (pH 8.0), 100 mM KCl, 5 mM MgCl₂, and 20% glycerol at 37 °C for 10 min. After incubation, each sample was loaded onto a 6% polyacrylamide native gel immediately after adding loading buffer. The gel was stained with ethidium bromide.

UV melting assays

UV melting assays were carried out as previously described (4, 80). The wildtype and mutant tRNA^{Met} transcripts were generated as described above. The tRNA^{Met} transcripts were diluted in the buffer including 50 mM sodium phosphate (pH 7.0), 50 mM NaCl, 5 mM MgCl₂, and 0.1 mM EDTA. Absorbance against temperature melting curves were measured at 260 nm with a heating rate of 0.5 °C/min from 25 to 95 °C through Agilent Cary 100 UV Spectrophotometer.

Mitochondrial tRNA analysis

For the tRNA Northern blot analysis, 2 μg of total mitochondrial RNAs were electrophoresed through a 10% polyacrylamide gel without (native gel) or with (denature gel) 8 M urea. The gels were then electroblotted onto a positively charged nylon membrane (Roche) for the hybridization analysis with specific DIG-labeled oligodeoxynucleotide tRNA^{Met} probe (21, 31, 81). After stripping, the same blots were hybridized with five DIG-labeled oligodeoxynucleotide tRNA probes in the following order: tRNA^{Lys}, tRNA^{Ser(UCN)}, tRNA^{Thr}, tRNA^{Leu(CUN)}, and tRNA^{Glu}, respectively. After hybridization, the membranes were washed with Washing buffer (0.1 M maleic acid, 0.15 M NaCl, 0.3% (v/v) Tween 20 (pH 7.5)), incubated for 30 min in Blocking solution (dilute blocking reagent (Roche) in 0.1 M maleic acid, 0.15 M NaCl (pH 7.5)), and then incubated for 30 min in Antibody solution (dilute anti-digoxigenin-AP Fab fragments (Roche), 1:10,000, in blocking solution). Anti-digoxigenin-AP Fab fragments for binding to the hybridized probes were used for the immunological detection. After incubation, the membranes were washed with 20 ml of washing buffer twice and equilibrated with detection buffer (0.1 M Tris-HCl, 0.1 M NaCl (pH 9.5)). CDP-Star, ready-to-use solution (Roche) was used to soak the membrane evenly before exposure and signals were detected using the ECL system (CW BIO). After exposure, the membranes were washed with sterile diethyl pyrocarbon-

ate-treated distilled water, incubated for 2 × 60 min at 80 °C in stripping buffer (50 mM Tris-HCl (pH 7.5), 50% formamide, 5% SDS), then washed for 2 × 5 min in 2 × SSC (300 mM NaCl, 30 mM sodium citrate (pH 7.0)) before prehybridization and hybridization with the next probe. To reduce the loss of tRNA during stripping, fresh stripping buffers were used for each time under sterile RNase-free conditions. The DIG-labeled oligodeoxynucleotides were generated by using a DIG oligonucleotide tailing kit (Roche). The hybridization and quantification of density in each band were performed as detailed previously (21, 31).

Oligodeoxynucleotides specific for tRNA^{Met}, tRNA^{Lys}, tRNA^{Ser(UCN)}, tRNA^{Thr}, tRNA^{Leu(CUN)}, and tRNA^{Glu} were as follows: 5'-TGGTAGTACGGGAAGGGTATAACCAACAT-T-3' (tRNA^{Met}), 5'-AAAGAGGTGTTGGTTCTCTTAATC-TTTAAC-3' (tRNA^{Lys}), 5'-AAAGGAAGGAATCGAACCC-CCAAAGCTGG-3' (tRNA^{Ser(UCN)}), 5'-TGTCCTTGAAAAAGGTTTTCATCTCCGG-3' (tRNA^{Thr}), 5'-ACTTTTATTTGGAGTTGCACCAAAATTTT-3' (tRNA^{Leu(CUN)}) and 5'-ATTCTCGCACGGACTACAACCACGACCAAT-3' (tRNA^{Glu}) (GenBankTM accession no. NC_001807) (5).

For the aminoacylation assays, total mitochondrial RNAs were isolated under acid conditions, and 2 μg of total mitochondrial RNAs was electrophoresed at 4 °C through an acid (pH 5.0) 10% PAGE with 8 M urea in 100 mM sodium acetate buffer to separate the charged and uncharged tRNA as detailed elsewhere (82, 83). To further distinguish nonaminoacylated tRNA from aminoacylated tRNA, total RNAs were treated with being heated for 10 min at 60 °C (pH 8.3) and then run in parallel (82, 83). The gels were then electroblotted as described above. Quantification of density in each band was performed as detailed previously (82, 83).

Western blot analysis

Western blotting analysis was performed as detailed elsewhere (44, 46). Antibodies were obtained from different companies including ND4 (sc-20499-R) from Santa Cruz Biotechnology, ATP6 (55313-1-AP), ATP8 (26723-1-AP), and CYTB (55090-1-AP) from Proteintech, CO₂ (ab110258), ND5 (ab92624), ND3 (ab170681), and Tom20 (ab56783) from Abcam. Peroxidase Affini Pure goat anti-mouse IgG and goat anti-rabbit IgG (Jackson) were used as a secondary antibody and protein signals were detected using the ECL system (CWBI). Quantification of density in each band was performed as detailed previously (44, 46).

Assays of activities of respiratory complexes

The enzymatic activities of complexes I, II, III, IV, and V were assayed as detailed before (40, 41).

Measurements of oxygen consumption

The OCR in cybrid cell lines were measured with a Seahorse Bioscience XF-96 extracellular flux analyzer (Seahorse Bioscience), as detailed previously (43, 44).

ATP measurements

The Cell Titer-Glo[®] Luminescent Cell Viability Assay kit (Promega) was used for the measurement of cellular and mito-

chondrial ATP levels, following the modified manufacturer's instructions (44, 46).

Assessment of mitochondrial membrane potential

Mitochondrial membrane potential was assessed with a JC-10 Assay Kit-Microplate (Abcam) according to the general manufacturer's recommendations with some modifications, as detailed elsewhere (44, 45).

Measurement of ROS production

ROS measurements were performed as detailed previously (29, 35, 47, 48).

Computer analysis

Statistical analysis was carried out using the unpaired, two-tailed Student's *t* test contained in the Microsoft-Excel program or Macintosh (version 2007). Differences were considered significant at *p* < 0.05.

Author contributions—M. Z., L. X., Y. C., H. L., Q. H., B. W., F. M., and M.-X. G. data curation; M. Z., L. X., and M.-X. G. formal analysis; M. Z. and M.-X. G. funding acquisition; M. Z., B. W., M. W., and M.-X. G. validation; M. Z., L. X., and Y. C. methodology; M. Z. and M.-X. G. writing-original draft; H. L. and M.-X. G. resources; Q. H. and M.-X. G. investigation; M. W. software; M.-X. G. conceptualization; M.-X. G. supervision; M.-X. G. project administration; M.-X. G. writing-review and editing.

Acknowledgments—We are grateful to Dr. En-Duo Wang (Shanghai Institute of Biochemistry and Cell Biology) for the pTrc99B-tRNA^{Leu(CAG)} and pTrc99B-tRNA^{Thr} plasmids and Dr. Shigeyuki Yokoyama (RIKEN Structural Biology Laboratory) for the pET26b-aTrm5 plasmid. We thank Dr. Gilbert Eriani (Institut de Biologie Moléculaire et Cellulaire) for the critical comments of this manuscript.

References

- Zhang, X., Cozen, A. E., Liu, Y., Chen, Q., and Lowe, T. M. (2016) Small RNA modifications: integral to function and disease. *Trends Mol. Med.* **22**, 1025–1034 [CrossRef Medline](#)
- Bohnsack, M. T., and Sloan, K. E. (2017) The mitochondrial epitranscriptome: the roles of RNA modifications in mitochondrial translation and human disease. *Cell Mol. Life Sci.* **75**, 241–260 [CrossRef Medline](#)
- Suzuki, T., Nagao, A., and Suzuki, T. (2011) Human mitochondrial tRNAs: biogenesis, function, structural aspects, and diseases. *Annu. Rev. Genet.* **45**, 299–329 [CrossRef Medline](#)
- Wang, M., Liu, H., Zheng, J., Chen, B., Zhou, M., Fan, W., Wang, H., Liang, X., Zhou, X., Eriani, G., Jiang, P., and Guan, M. X. (2016) A deafness- and diabetes-associated trna mutation causes deficient pseudouridylation at position 55 in tRNA^{Glu} and mitochondrial dysfunction. *J. Biol. Chem.* **291**, 21029–21041 [CrossRef Medline](#)
- Andrews, R. M., Kubacka, I., Chinnery, P. F., Lightowlers, R. N., Turnbull, D. M., and Howell, N. (1999) Reanalysis and revision of the Cambridge reference sequence for human mitochondrial DNA. *Nat. Genet.* **23**, 147 [CrossRef Medline](#)
- Phizicky, E. M., and Hopper, A. K. (2010) tRNA biology charges to the front. *Genes Dev.* **24**, 1832–1860 [CrossRef Medline](#)
- El Yacoubi, B., Bailly, M., and de Crécy-Lagard, V. (2012) Biosynthesis and function of posttranscriptional modifications of transfer RNAs. *Annu. Rev. Genet.* **46**, 69–95 [CrossRef Medline](#)
- Hori, H. (2014) Methylated nucleosides in tRNA and tRNA methyltransferases. *Front. Genet.* **5**, 144 [Medline](#)

9. Suzuki, T., and Suzuki, T. (2014) A complete landscape of post-transcriptional modifications in mammalian mitochondrial tRNAs. *Nucleic Acids Res.* **42**, 7346–7357 [CrossRef Medline](#)
10. Machnicka, M. A., Milanowska, K., Osman Oglou, O., Purta, E., Kurkowska, M., Olchowik, A., Januszewski, W., Kalinowski, S., Dunin-Horkawicz, S., Rother K. M., *et al.* (2013) MODOMICS: a database of RNA modification pathways: 2013 update. *Nucleic Acids Res.* **41**, D262–D267 [Medline](#)
11. Bjork, G. R. (1995) Genetic dissection of synthesis and function of modified nucleosides in bacterial transfer RNA. *Prog. Nucleic Acids Res. Mol. Biol.* **50**, 263–338 [CrossRef](#)
12. Väre, V. Y., Eruysal, E. R., Narendran, A., Sarachan, K. L., and Agris, P. F. (2017) Chemical and conformational diversity of modified nucleosides affects tRNA structure and function. *Biomolecules* **7**, pii: E29
13. Helm, M., Brulé, H., Degoul, F., Cepanec, C., Leroux, J. P., Giegé, R., and Florentz, C. (1998) The presence of modified nucleotides is required for cloverleaf folding of a human mitochondrial tRNA. *Nucleic Acids Res.* **26**, 1636–1643 [CrossRef Medline](#)
14. Gingold, H., and Pilpel, Y. (2011) Determinants of translation efficiency and accuracy. *Mol. Syst. Biol.* **7**, 481 [Medline](#)
15. Allnér, O., and Nilsson, L. (2011) Nucleotide modifications and tRNA anticodon-mRNA codon interactions on the ribosome. *RNA* **17**, 2177–2188 [CrossRef Medline](#)
16. Drummond, D. A., and Wilke, C. O. (2008) Mistranslation-induced protein misfolding as a dominant constraint on coding-sequence evolution. *Cell* **134**, 341–352 [CrossRef Medline](#)
17. Johansson, M. J., Esberg, A., Huang, B., Björk, G. R., and Byström, A. S. (2008) Eukaryotic wobble uridine modifications promote a functionally redundant decoding system. *Mol. Cell. Biol.* **28**, 3301–3312 [CrossRef Medline](#)
18. Kirino, Y., Goto, Y., Campos, Y., Arenas, J., and Suzuki, T. (2005) Specific correlation between the wobble modification deficiency in mutant tRNAs and the clinical features of a human mitochondrial disease. *Proc. Natl. Acad. Sci. U.S.A.* **102**, 7127–7132 [CrossRef Medline](#)
19. Yasukawa, T., Suzuki, T., Ueda, T., Ohta, S., and Watanabe, K. (2000) Modification defect at anticodon wobble nucleotide of mitochondrial tRNA^{Leu(UUR)} with pathogenic mutations of mitochondrial myopathy, encephalopathy, lactic acidosis, and stroke-like episodes. *J. Biol. Chem.* **275**, 4251–4257 [CrossRef Medline](#)
20. Yasukawa, T., Suzuki, T., Ishii, N., Ohta, S., and Watanabe, K. (2001) Wobble modification defect in tRNA disturbs codon-anticodon interaction in a mitochondrial disease. *EMBO J.* **20**, 4794–4802 [CrossRef Medline](#)
21. Guan, M. X., Yan, Q., Li, X., Bykhovskaya, Y., Gallo-Teran, J., Hajek, P., Umeda, N., Zhao, H., Garrido, G., Mengesha, E., *et al.* (2006) Mutation in TRMU related to transfer RNA modification modulates the phenotypic expression of the deafness-associated mitochondrial 12S ribosomal RNA mutations. *Am. J. Hum. Genet.* **79**, 291–302 [CrossRef Medline](#)
22. Meng, F., Cang, X., Peng, Y., Li, R., Zhang, Z., Li, F., Fan, Q., Guan, A. S., Fischel-Ghoshian, N., Zhao, X., and Guan, M. X. (2017) Biochemical evidence for a nuclear modifier allele (A10S) in TRMU (Methylaminomethyl-2-thiouridylyltransferase) related to mitochondrial tRNA modification in the phenotypic manifestation of deafness-associated 12S rRNA mutation. *J. Biol. Chem.* **292**, 2881–2892 [CrossRef Medline](#)
23. Kopajtich, R., Nicholls, T. J., Rorbach, J., Metodiev, M. D., Freisinger, P., Mandel, H., Vanlander, A., Ghezzi, D., Carrozzo, R., Taylor, R. W., Marquard, K., *et al.* (2014) Mutations in GTPBP3 cause a mitochondrial translation defect associated with hypertrophic cardiomyopathy, lactic acidosis, and encephalopathy. *Am. J. Hum. Genet.* **95**, 708–720 [CrossRef Medline](#)
24. Ghezzi, D., Baruffini, E., Haack, T. B., Invernizzi, F., Melchionda, L., Dallabona, C., Strom, T. M., Parini, R., Burlina, A. B., Meitinger, T., Prokisch, H., Ferrero, I., and Zeviani, M. (2012) Mutations of the mitochondrial-tRNA modifier MTO1 cause hypertrophic cardiomyopathy and lactic acidosis. *Am. J. Hum. Genet.* **90**, 1079–1087 [CrossRef Medline](#)
25. Van Haute, L., Dietmann, S., Kremer, L., Hussain, S., Pearce, S. F., Powell, C. A., Rorbach, J., Lantaff, R., Blanco, S., Sauer, S., *et al.* (2016) Deficient methylation and formylation of mt-tRNA^{Met} wobble cytosine in a patient carrying mutations in NSUN3. *Nat. Commun.* **7**, 12039 [CrossRef Medline](#)
26. Yarham, J. W., Lamichhane, T. N., Pyle, A., Mattijssen, S., Baruffini, E., Bruni, F., Donnini, C., Vassilev, A., He, L., Blakely, E. L., *et al.* (2014) Defective i6A37 modification of mitochondrial and cytosolic tRNAs results from pathogenic mutations in TRIT1 and its substrate tRNA. *PLoS Genet.* **10**, e1004424 [CrossRef Medline](#)
27. Powell, C. A., Kopajtich, R., D'Souza, A. R., Rorbach, J., Kremer, L. S., Husain, R. A., Dallabona, C., Donnini, C., Alston, C. L., Griffin, H., *et al.* (2015) TRMT5 mutations cause a defect in post-transcriptional modification of mitochondrial tRNA associated with multiple respiratory-chain deficiencies. *Am. J. Hum. Genet.* **97**, 319–328 [CrossRef Medline](#)
28. Wang, M., Peng, Y., Zheng, J., Zheng, B., Jin, X., Liu, H., Wang, Y., Tang, X., Huang, T., Jiang, P., and Guan, M. X. (2016) A deafness-associated tRNA^{ASP} mutation alters the m1G37 modification, aminoacylation and stability of tRNA^{ASP} and mitochondrial function. *Nucleic Acids Res.* **44**, 10974–10985 [CrossRef Medline](#)
29. Merante, F., Myint, T., Tein, I., Benson, L., and Robinson, B. H. (1986) An additional mitochondrial tRNA^{Leu} point mutation (A-to-G at nucleotide 4295) causing hypertrophic cardiomyopathy. *Hum. Mutat.* **8**, 216–222 [Medline](#)
30. Qu, J., Li, R., Tong, Y., Lu, F., Qian, Y., Hu, Y., Mo, J. Q., West, C. E., and Guan, M. X. (2006) The novel A4435G mutation in the mitochondrial tRNA^{Met} may modulate the phenotypic expression of the LHON-associated ND4 G11778A mutation. *Invest. Ophthalmol. Vis. Sci.* **47**, 475–483
31. Liu, Y., Li, R., Li, Z., Wang, X. J., Yang, L., Wang, S., and Guan, M. X. (2009) Mitochondrial transfer RNA^{Met} 4435A>G mutation is associated with maternally inherited hypertension in a Chinese pedigree. *Hypertension.* **53**, 1083–1090 [CrossRef Medline](#)
32. Lu, Z., Chen, H., Meng, Y., Wang, Y., Xue, L., Zhi, S., Qiu, Q., Yang, L., Mo, J. Q., and Guan, M. X. (2011) The tRNA^{Met} 4435A>G mutation in the mitochondrial haplogroup G2a1 is responsible for maternally inherited hypertension in a Chinese pedigree. *Eur. J. Hum. Genet.* **19**, 1181–1186 [CrossRef Medline](#)
33. Xue, L., Wang, M., Li, H., Wang, H., Jiang, F., Hou, L., Geng, J., Lin, Z., Peng, Y., Zhou, H., Yu, H., Jiang, P., Mo, J. Q., and Guan, M. X. (2016) Mitochondrial tRNA mutations in 2070 Chinese Han subjects with hypertension. *Mitochondrion.* **30**, 208–221 [CrossRef Medline](#)
34. King, M. P., and Attadi, G. (1996) Mitochondria-mediated transformation of human rho(0) cells. *Methods Enzymol.* **264**, 313–334 [CrossRef Medline](#)
35. Jiang, P., Wang, M., Xue, L., Xiao, Y., Yu, J., Wang, H., Yao, J., Liu, H., Peng, Y., Liu, H., Li, H., Chen, Y., and Guan, M. X. (2016) A hypertension-associated tRNA^{Ala} mutation alters tRNA metabolism and mitochondrial function. *Mol. Cell. Biol.* **36**, 1920–1930 [CrossRef Medline](#)
36. Goto-Ito, S., Ito, T., Ishii, R., Muto, Y., Bessho, Y., and Yokoyama, S. (2008) Crystal structure of archaeal tRNA m¹G37 methyltransferase aTrm5. *Proteins* **72**, 1274–1289 [CrossRef Medline](#)
37. Goto-Ito, S., Ito, T., and Yokoyama, S. (2017) Trm5 and TrmD: two enzymes from distinct origins catalyze the identical tRNA modification, m¹G37. *Biomolecules* **7**, E32 [Medline](#)
38. Ojala, D., Montoya, J., and Attardi, G. (1981) tRNA punctuation model of RNA processing in human mitochondria. *Nature* **290**, 470–474 [CrossRef Medline](#)
39. Guan, M. X., Enriquez, J. A., Fischel-Ghoshian, N., Puranam, R. S., Lin, C. P., Maw, M. A., and Attardi, G. (1998) The deafness-associated mitochondrial DNA mutation at position 7445, which affects tRNA^{Ser(UCN)} precursor processing, has long-range effects on NADH dehydrogenase subunit ND6 gene expression. *Mol. Cell. Biol.* **18**, 5868–5879 [CrossRef Medline](#)
40. Li, Y., D'Aurelio, M., Deng, J. H., Park, J. S., Manfredi, G., Hu, P., Lu, J., and Bai, Y. (2007) An assembled complex IV maintains the stability and activity of complex I in mammalian mitochondria. *J. Biol. Chem.* **282**, 17557–17562 [CrossRef Medline](#)
41. Thorburn, D. R., Chow, C. W., and Kirby, D. M. (2004) Respiratory chain enzyme analysis in muscle and liver. *Mitochondrion* **4**, 363–375 [CrossRef Medline](#)

42. Scheffler, I. E. (2015) Mitochondrial disease associated with complex I (NADH-CoQ oxidoreductase) deficiency. *J. Inher. Metab. Dis.* **38**, 405–415 [CrossRef](#)
43. Dranka, B. P., Benavides, G. A., Diers, A. R., Giordano, S., Zelickson, B. R., Reily, C., Zou, L., Chatham, J. C., Hill, B. G., Zhang, J., Landar, A., and Darley-Usmar, V. M. (2011) Assessing bioenergetic function in response to oxidative stress by metabolic profiling. *Free Radic. Biol. Med.* **51**, 1621–1635 [CrossRef Medline](#)
44. Gong, S., Peng, Y., Jiang, P., Wang, M., Fan, M., Wang, X., Zhou, H., Li, H., Yan, Q., Huang, T., and Guan, M. X. (2014) A deafness-associated tRNA^{His} mutation alters the mitochondrial function, ROS production and membrane potential. *Nucleic Acids Res.* **42**, 8039–8048 [CrossRef Medline](#)
45. Reers, M., Smiley, S. T., Mottola-Hartshorn, C., Chen, A., Lin, M., and Chen, L. B. (1995) Mitochondrial membrane potential monitored by JC-1 dye. *Methods Enzymol.* **260**, 406–417 [CrossRef Medline](#)
46. Jiang, P., Jin, X., Peng, Y., Wang, M., Liu, H., Liu, X., Zhang, Z., Ji, Y., Zhang, J., Liang, M., et al. (2016) The exome sequencing identified the mutation in YARS2 encoding the mitochondrial tyrosyl-tRNA synthetase as a nuclear modifier for the phenotypic manifestation of Leber's hereditary optic neuropathy-associated mitochondrial DNA mutation. *Hum. Mol. Genet.* **25**, 584–596 [CrossRef Medline](#)
47. Zhang, J., Liu, X., Liang, X., Lu, Y., Zhu, L., Fu, R., Ji, Y., Fan, W., Chen, J., Lin, B., et al. (2017) A novel ADOA-associated OPA1 mutation alters the mitochondrial function, membrane potential, ROS production and apoptosis. *Sci. Rep.* **7**, 5704 [CrossRef Medline](#)
48. Mahfouz, R., Sharma, R., Lackner, J., Aziz, N., and Agarwal, A. (2009) Evaluation of chemiluminescence and flow cytometry as tools in assessing production of hydrogen peroxide and superoxide anion in human spermatozoa. *Fertil. Steril.* **92**, 819–827 [CrossRef Medline](#)
49. Nakano, S., Suzuki, T., Kawarada, L., Iwata, H., Asano, K., and Suzuki, T. (2016) NSUN3 methylase initiates 5-formylcytidine biogenesis in human mitochondrial tRNA^{Met}. *Nat. Chem. Biol.* **12**, 546–551 [CrossRef Medline](#)
50. Bjork, G. R., and Hagervall, T. G. (2014) Transfer RNA modification: presence, synthesis, and function. *EcoSal Plus* **6**, 10.1128/ecosalplus
51. Florentz, C., Sohm, B., Tryoen-Tóoth, P., Pütz, J., and Sissler, M. (2003) Human mitochondrial tRNAs in health and disease. *Cell Mol. Life Sci.* **60**, 1356–1375 [CrossRef Medline](#)
52. Buck, M., and Griffiths, E. (1982) Iron mediated methylthiolation of tRNA as a regulator of operon expression in *Escherichia coli*. *Nucleic Acids Res.* **10**, 2609–2624 [CrossRef](#)
53. Urbonavicius, J., Qian, Q., Durand, J. M., Hagervall, T. G., and Björk, G. R. (2001) Improvement of reading frame maintenance is a common function for several tRNA modifications. *EMBO J.* **20**, 4863–4873 [CrossRef Medline](#)
54. Yarus, M., Cline, S. W., Wier, P., Breeden, L., and Thompson, R. C. (1986) Actions of the anticodon arm in translation on the phenotypes of RNA mutants. *J. Mol. Biol.* **192**, 235–255 [CrossRef Medline](#)
55. Li, X., Fischel-Ghodsian, N., Schwartz, F., Yan, Q., Friedman, R. A., and Guan, M. X. (2004) Biochemical characterization of the mitochondrial tRNA^{Ser(U^{CN})} T7511C mutation associated with nonsyndromic deafness. *Nucleic Acids Res.* **32**, 867–877 [CrossRef Medline](#)
56. Wang, S., Li, R., Fettermann, A., Li, Z., Qian, Y., Liu, Y., Wang, X., Zhou, A., Mo J. Q., Yang L., Jiang, P., Taschner, A., Rossmann, W., and Guan, M. X. (2011) Maternally inherited essential hypertension is associated with the novel 4263A>G mutation in the mitochondrial tRNA^{Ala} gene in a large Han Chinese family. *Circ. Res.* **108**, 862–870 [CrossRef Medline](#)
57. Masucci, J. P., Davidson, M., Koga, Y., Schon, E. A., and King, M. P. (1995) *In vitro* analysis of mutations causing myoclonus epilepsy with ragged-red fibers in the mitochondrial tRNA^{Lys} gene: two genotypes produce similar phenotypes. *Mol. Cell. Biol.* **15**, 2872–2881 [CrossRef Medline](#)
58. Enriquez, J. A., Chomyn, A., and Attardi, G. (1995) MtDNA mutation in MERRF syndrome causes defective aminoacylation of tRNA^{Lys} and premature translation termination. *Nat. Genet.* **10**, 47–55 [CrossRef Medline](#)
59. Wallace, D. C. (2005) A mitochondrial paradigm of metabolic and degenerative diseases, aging, and cancer: a dawn for evolutionary medicine. *Annu. Rev. Genet.* **39**, 359–407 [CrossRef Medline](#)
60. Hayashi, G., and Cortopassi, G. (2015) Oxidative stress in inherited mitochondrial diseases. *Free Radic. Biol. Med.* **88**, 10–17 [CrossRef Medline](#)
61. Schieber, M., and Chandel, N. S. (2014) ROS function in redox signaling and oxidative stress. *Curr. Biol.* **24**, R453–R462 [CrossRef Medline](#)
62. Addabbo, F., Montagnani, M., and Goligorsky, M. S. (2009) Mitochondria and reactive oxygen species. *Hypertension* **53**, 885–892 [CrossRef Medline](#)
63. Eirin, A., Lerman, A., and Lerman, L. O. (2015) Mitochondria: a pathogenic paradigm in hypertensive renal disease. *Hypertension* **65**, 264–270 [CrossRef Medline](#)
64. Vasani, R. S., Beiser, A., Seshadri, S., Larson, M. G., Kannel, W. B., D'Agostino, R. B., and Levy, D. (2002) Residual lifetime risk for developing hypertension in middle-aged women and men: The Framingham Heart Study. *JAMA* **287**, 1003–1010 [Medline](#)
65. Archer, S. L., Marsboom, G., Kim, G. H., Zhang, H. J., Toth, P. T., Svensson, E. C., Dyck, J. R., Gombert-Maitland, M., Thébaud, B., Husain, A. N., Cipriani, N., and Rehman, J. (2010) Epigenetic attenuation of mitochondrial superoxide dismutase 2 in pulmonary arterial hypertension: a basis for excessive cell proliferation and a new therapeutic target. *Circulation* **121**, 2661–2671 [CrossRef Medline](#)
66. Dittmar, K. A., Goodenbour, J. M., and Pan, T. (2006) Tissue-specific differences in human transfer RNA expression. *PLoS Genet.* **2**, e221 [CrossRef Medline](#)
67. Tischner, C., Hofer, A., Wulff, V., Stepek, J., Dumitru, I., Becker, L., Haack, T., Kremer, L., Datta, A. N., Sperl, W., et al. (2015) MTO1 mediates tissue specificity of OXPHOS defects via tRNA modification and translation optimization, which can be bypassed by dietary intervention. *Hum. Mol. Genet.* **24**, 2247–2266 [CrossRef Medline](#)
68. Powell, C. A., Nicholls, T. J., and Minczuk, M. (2015) Nuclear-encoded factors involved in post-transcriptional processing and modification of mitochondrial tRNAs in human disease. *Front. Genet.* **6**, 79 [CrossRef Medline](#)
69. Chen, D., Li, F., Yang, Q., Tian, M., Zhang, Z., Zhang, Q., Chen, Y., and Guan, M. X. (2016) The defective expression of gtpbp3 related to tRNA modification alters the mitochondrial function and development of zebrafish. *Int. J. Biochem. Cell Biol.* **77**, 1–9 [CrossRef Medline](#)
70. Miller, G., and Lipman, M. (1973) Release of infectious Epstein-Barr virus by transformed marmoset leukocytes. *Proc. Natl. Acad. Sci. U.S.A.* **70**, 190–194 [CrossRef Medline](#)
71. King, M. P., and Attardi, G. (1989) Human cells lacking mtDNA: repopulation with exogenous mitochondria by complementation. *Science* **246**, 500–503 [CrossRef Medline](#)
72. Ofengand, J., Del Campo, M., and Kaya, Y. (2001) Mapping pseudouridines in RNA molecules. *Methods* **25**, 365–373 [CrossRef Medline](#)
73. Qian, Y., and Guan, M. X. (2009) Interaction of aminoglycosides with human mitochondrial 12S rRNA carrying the deafness-associated mutation. *Antimicrob. Agents Chemother.* **53**, 4612–4618 [CrossRef Medline](#)
74. King, M. P., and Attardi, G. (1993) Post-transcriptional regulation of the steady-state levels of mitochondrial tRNAs in HeLa cells. *J. Biol. Chem.* **268**, 10228–10237 [Medline](#)
75. Long, T., Li, J., Li, H., Zhou, M., Zhou, X. L., Liu, R. J., and Wang, E. D. (2016) Sequence-specific and shape-selective RNA recognition by the human RNA 5-methylcytosine methyltransferase NSun6. *J. Biol. Chem.* **291**, 24293–24303 [CrossRef Medline](#)
76. Li, Y., Chen, J., Wang, E., and Wang, Y. (1999) T7 RNA polymerase transcription of *Escherichia coli* isoacceptors tRNA^{Leu}. *Sci. China Ser. C* **42**, 185–190 [CrossRef](#)
77. Bonnefond, L., Fender, A., Rudinger-Thirion, J., Giegé, R., Florentz, C., and Sissler, M. (2005) Toward the full set of human mitochondrial aminoacyl-tRNA synthetases: characterization of AspRS and TyrRS. *Biochemistry* **44**, 4805–4816 [CrossRef Medline](#)
78. Watanabe, K., Nureki, O., Fukai, S., Ishii, R., Okamoto, H., Yokoyama, S., Endo, Y., and Hori, H. (2005) Roles of conserved amino acid sequence motifs in the SpoU (TrmH) RNA methyltransferase family. *J. Biol. Chem.* **280**, 10368–10377 [CrossRef Medline](#)
79. Zhou, M., Long, T., Fang, Z. P., Zhou, X. L., Liu, R. J., and Wang, E. D. (2015) Identification of determinants for tRNA substrate recognition by *Escherichia coli* C/US4 2'-O-methyltransferase. *RNA Biol.* **12**, 900–911 [CrossRef Medline](#)
80. Zhou, M., Wang, M., Xue, L., Lin, Z., He, Q., Shi, W., Chen, Y., Jin, X., Li, H., Jiang, P., and Guan, M. X. (2017) A hypertension-associated mitochon-

Hypertension-linked mitochondrial tRNA^{Met} mutation

- drial DNA mutation alters the tertiary interaction and function of tRNA^{Leu(UUR)}. *J. Biol. Chem.* **292**, 13934–13946 [CrossRef Medline](#)
81. Wang, X., Lu, J., Zhu, Y., Yang, A., Yang, L., Li, R., Chen, B., Qian, Y., Tang, X., Wang, J., Zhang, X., and Guan, M. X. (2008) Mitochondrial tRNA^{Thr} G15927A mutation may modulate the phenotypic manifestation of ototoxic 12S rRNA A1555G mutation in four Chinese families. *Pharmacogenet. Genomics* **18**, 1059–1070 [CrossRef Medline](#)
82. Enríquez, J. A., and Attardi, G. (1996) Analysis of aminoacylation of human mitochondrial tRNAs. *Methods Enzymol.* **264**, 183–196 [CrossRef Medline](#)
83. Li, R., and Guan, M. X. (2010) Human mitochondrial leucyl-tRNA synthetase corrects mitochondrial dysfunctions due to the tRNA^{Leu(UUR)} A3243G mutation, associated with mitochondrial encephalomyopathy, lactic acidosis, and stroke-like symptoms and diabetes. *Mol. Cell. Biol.* **30**, 2147–2154 [CrossRef Medline](#)